Vertical mixing in the marginal ice zone of the Barents Sea

Spatial and temporal variation of oceanic turbulence
- observations and numerical model experiments

Arild Sundfjord

Dissertation for the degree philosophiae doctor (PhD)
at the University of Bergen

January 2007

Abstract

Vertical mixing affects water mass modification, biological productivity, and chemical fluxes in the ocean, but its response to forcing and variability in time and space in seasonally ice-covered seas is inadequately known. As part of an interdisciplinary project, CABANERA, drop-sonde microstructure measurements were made during ice drift stations in the marginal ice zone (MIZ) of the northern Barents Sea in 2004 and 2005. Turbulent diffusivity rates in the surface mixed layer, pycnocline, and deeper stratified waters, inferred from the measurements, were found to vary greatly. Concurrent observations of fine-scale currents and wind, and predictions from a tidal model allowed for events of enhanced turbulence to be attributed to wind episodes and strong tides, and relationships explaining e.g. the upper-ocean vertical distribution of diffusivity as function of wind speed to be established. The large measured dissipation values were supported through independent estimates of water column overturning scales. In low-energy areas in the interior MIZ, double diffusive convection was found to produce significant heat fluxes.

The processes producing and dissipating turbulent energy are not fully understood, and the added complexity of the variable ice cover in the MIZ aggravates the challenges associated with prediction and modelling of turbulence in this region. In this study we performed model simulations of ice and ocean dynamics for the three project years, with a special emphasis on vertical mixing. Large-scale features such as inflow of Atlantic Water and exchange of ice with the adjacent seas are described and compared with available observations. The seasonal development of diffusivity and stratification is presented, from the vertically near-homogeneous winter situation through the highly stratified melting season and into the ice-free summer. Differences between two mixing parameterization schemes are explored, and benefits of increasing both horizontal and vertical model grid resolution are identified. Finally, adaptations to improve the performance of the mixing parameterizations in MIZ applications are suggested.

Acknowledgements

Many thanks to my supervisors, Prof. Harald Svendsen at the Geophysical Institute, University of Bergen, and Prof. Paul Wassmann at the College of Fishery Science, University of Tromsø, for their trust and guidance throughout the project. I am also very grateful for the collaboration with scientists at the Geophysical Institute/Bjerknes Centre for Climate Research, University of Bergen; first and foremost Dr. Ilker Fer, without whom the turbulence micro-scale measurements and analysis would not have been made. Pierre Jaccard, Steinar Myking, Yoshie Kasajima and Karolina Widell have also contributed in different ways – thanks! Also in Bergen, at the Institute of Marine Research, Randi Ingvaldsen and Jan Erik Stiansen have provided useful input. Thanks to Frank Nilsen who has made visits at UNIS, Longyearbyen, fruitful in several ways. Dag Slagstad and Ingrid Ellingsen at SINTEF, Trondheim, have provided numerical modelling expertise and answered questions of all sorts, thanks for the patience!

To my colleagues in Tromsø: Stig Falk-Petersen, Nalân Koç and everyone in the Physical Oceanography group at the Norwegian Polar Institute, with particular thanks to Vigdis Tverberg, Ole Anders Nøst, Signe Aaboe and Jofrid Skarðhamar (Akvaplan-niva) for reading and discussing premature manuscripts; Marit Reigstad, Else Nøst Hegseth and others at the College of Fishery Science, University of Tromsø; fellow PhD-students Tobias, Signe, Janne, Christian; all other CABANERA friends – it's been a good time!

I thank Eddy Carmack, Bill Williams, Lisa Miller and Conrad Cooper for hosting a most pleasant visit at the Institute of Ocean Sciences, Sydney, BC, Canada. Tom Weingartner, Zygmund Kowalik and Markus Janout made my stay at the Institute of Marine Science, University of Alaska Fairbanks, Fairbanks, AK, USA, useful and fun.

Finally, thanks to Lars G. Golmen and Torbjørn M. Johnsen at NIVA-Bergen for getting me started, and Kari Nygaard, NIVA-Oslo, for encouraging me to go for this project.

Thanks also to those of you who entrusted me with instrumentation for the field work. You shouldn't have.

The research has been funded by the Research Council of Norway under the NORKLIMA project CABANERA (grant no 155936/S30). Travel support to IOS, BC, Canada, and UAF, AK, USA, was provided by the Research Council of Norway as a personal foreign exchange grant. CPUs at the supercomputing cluster Snowstorm at the University of Tromsø were allocated through the NOTUR programme. Thanks also to the Norwegian Polar Institute for the grant 'Arktisstipend' supporting field work in Kongsfjorden, Svalbard.

List of papers

Sundfjord, A., I. Fer, Y. Kasajima and H. Svendsen, 2006. Observations of turbulent mixing and hydrography in the marginal ice zone of the Barents Sea. Journal of Geophysical Research - Oceans, in press.

Fer, I. and A. Sundfjord, 2006. Observations of upper ocean boundary layer dynamics in the marginal ice zone. Journal of Geophysical Research - Oceans, in press.

Sundfjord, A., I. Ellingsen, D. Slagstad and H. Svendsen, 2006. Vertical mixing in the MIZ of the Barents Sea – results from numerical model experiments. Deep Sea Research-II, accepted.

Introduction

Contents

1. Introduction

The main topic of this thesis is upper-ocean turbulence and associated vertical mixing, with focus on the marginal ice zone (MIZ) of the Barents Sea. Apart from being an interesting and challenging fundamental physical process in its own right, turbulence is important for the development of mixed layers and pycnoclines, and it regulates vertical heat fluxes thus modifying the growth and decay of sea ice. Turbulence also affects biological activity and vertical transports of chemical constituents. On larger scales, turbulence controls the exchange between surface and deep waters by converting vast amounts of energy from wind and tides to potential energy, and so influences the main current systems of the world oceans.

Although extensively studied, the mechanisms controlling the distribution of turbulence intensity in time and space are not fully understood, and are difficult to predict. Many studies of oceanic turbulence have been made in the deep open ocean, in attempts to reconcile the budget of mean diffusivity required to maintain observed stratification and of the energy providing this mixing (Gregg, 1987; Munk, 1966). To this end, considerable effort has been put into investigations of the coupling between breaking internal waves and turbulence (Gregg, 1989), and enhanced mixing over rough seafloor topography (Polzin et al., 1997). The effect of breaking surface waves on the mixed layer has also been shown increasing attention in recent years (Craig and Banner, 1994; Ezer, 2000; Mellor, 2003; Qiao et al., 2004). Many studies of turbulent mixing have also been performed in coastal environments like channels and fjords (Gargett and Moum, 1995), and on continental shelves (Simpson et al., 1996) and shelf slopes (Sharples et al., 2001). Although some investigations have focussed on ice covered waters, these studies have mostly been in the deep ocean (e.g. Morison et al., 1987; Padman and Dillon, 1991) or under land-fast ice (Crawford et al., 1999). How drifting sea ice in shallow and topographically complex areas affects the distribution of turbulence is still poorly known and requires more study. The present study can hopefully help improve our understanding of these processes.

The work described in the following focuses primarily on the upper part of the water column; the surface mixed layer, the pycnocline and the stratified waters immediately below the pycnocline. Processes regulating water mass modification, biological productivity and marine chemistry mostly occur in this depth interval, typically the upper ~50 m. Several laboratory and mesocosm studies have investigated the coupling between turbulence and biological activity; this project is one of a modest number where these processes are studied in concert in the field.

The difficulties in describing and understanding turbulence in nature are reflected in the way it is treated in numerical ocean models. Closing the gap between physical processes and the representation of them in models is also a field of continuous development. It is the aim of this project to contribute to the improvement of turbulence modelling by providing in situ data applicable for model evaluation.

Our study area, the Barents Sea, has supported abundant fisheries for centuries, and with the recent advances in harvesting technology the need for holistic resource management has become evident. Ongoing exploration, extraction and export of hydrocarbons from the area requires knowledge of the physical environment, including ice conditions, which poses new challenges for the oil and gas industry as it continues to move further north. Numerical ocean models are the only tools capable of integrating all the processes that interact to produce the environment of this complex area. Oceanic mixing processes must be properly understood and represented in the models to get stratification and vertical transports correct – fundamental for simulating both biological productivity and e.g. sea ice cover development.

The Barents Sea is a frontal zone between the Atlantic water regime and the deep Arctic Ocean; incoming Atlantic Water (AW) conveys large amounts of heat and salt while cold, less saline water is brought in with Arctic Water (ArW) and sea ice. As these waters meet and mix, their characteristics change and new strata with different properties are formed. Changes to this atmosphere-ice-ocean system, as suggested by climate models, may have consequences well beyond the Barents Sea itself.

While much is known about the southern part of the Barents Sea, e.g. variability of the inflow of AW and seasonal development of stratification, the northern part is less explored. North of the Polar Front, scientific undertakings have mostly been confined to the summer months when the ice edge recedes. The dynamics in the MIZ are important as the processes here influence the stratification for the following productive season. Also, processes in the MIZ have the potential of producing intermediate depth waters for export to the deep Arctic Ocean, where these can act as insulation for the AW trapped below the cold surface layer. Biological production is known to be very high along the receding ice edge in spring and summer, and the ecosystem dynamics of large areas will be different if the ice-free areas of the Barents Sea become more extensive in a warmer climate. Knowledge gained from the Barents Sea MIZ can be applicable for the other Artic shelf seas, as well as the Arctic Ocean proper.

2. The Cabanera project

The work described in this thesis is part of the CABANERA project ('Carbon flux and ecosystem feed back in the northern Barents Sea in an era of climate change'), funded by the Research Council of Norway's NORKLIMA programme. The project studies the biological, chemical and physical components of the marine carbon cycle in an integrated manner. Three vessel-based cruises have been made in 2003-2005, covering different parts of the central and northern Barents Sea during different settings of ice cover, phytoplankton blooms and at different stages of the summer season. Lower-trophic-level biology from bacteria to phytoplankton and zooplankton, and from sympagic (ice associated) via pelagic to benthic species, was studied at ice drift stations typically lasting 1.5 day each. Vertical fluxes of particulate organic matter as well as concentrations of dissolved nutrients and carbon system constituents were measured. In addition, physical oceanographical data collection comprising CTD data, ADCP current measurements and microstructure profiling was made. CTD and ADCP data were also collected during two similar cruises organized by the 'On Thin Ice?' project (Research Council of Norway).

Given that the extent of the ice cover varies primarily with a) the relative contributions of incoming warm Atlantic Water and cold Arctic Water, b) ice extent of the previous year, c) the depth of the winter mixed layer and d) the pathways of low-pressure systems, some of the basic hypotheses of the project are:

1) Gross primary production varies with the extent of the ice cover, with less production and a larger relative contribution from ice algae than pelagic species in years with more ice.

2) Deeper vertical mixing associated with ice free areas will increase the pelagic retention of primary production, whereas stronger stratification and sympagic dominance will give more rapid export to benthos.

3) The competing effects of increased primary production and retention versus smaller productivity and rapid export imply that the net carbon sedimentation might not increase despite larger ice-free shelf areas.

4) Winter mixed layer depth influences the degree of sequestration of dissolved carbon; shelf areas where the winter mixed layer reaches the bottom will be more efficient for net CO_2 uptake.

The interactions of the processes covered in the measurement campaign are integrated in a numerical model, SINMOD. This three-dimensional hydrodynamical model system contains a comprehensive lower-trophic-level biological module specifically designed for the region. Carbon fluxes are followed through the biological cycles and in dissolved state, and the amounts of e.g. new production and sedimentation can be assessed.

3. Main objectives

The physical oceanography component of the Cabanera project provides a tool for interpretation and integration of results from the other modules. There are also specific goals for increased fundamental process knowledge, with particular focus on vertical mixing. The main objectives can be summarized as follows:

1) Description of physical 'status' during ice drift stations, for interpretation of bio-geo-measurements. This includes assessing the evolution of the water column at the stations preceding the measurements; temporal development of mixing and stratification, and water mass pathways and origins. Paper 1 in this thesis addresses these issues, as well as two manuscripts not included here[1].

2) Increase the basic knowledge of vertical mixing processes in the MIZ. This includes describing how a partial ice cover influences turbulent mixing compared with open ocean locations; e.g. the vertical distribution of turbulent kinetic energy in response to wind episodes and changing tidal current shear profiles. Also, identify other mixing processes such as cross-frontal mixing, upwelling and double diffusion. These are the topics of Papers 1 and 2.

3) Integrate the acquired knowledge in an assessment of the vertical mixing scheme of the numerical ocean model used in the project. Based on this, suggest improvements to the model (Paper 3).

---

[1] Kivimäe, C., R. Bellerby, A. Sundfjord and A. M. Omar. Variability of new production and CO_2 air-sea exchange in the north-western Barents Sea in relation to sea ice cover. Submitted to Journal of Marine Research, Sept. 2006.

Hegseth, E. N. and A. Sundfjord. Intrusion and blooming of Atlantic phytoplankton species in the high Arctic. Submitted to Journal of Marine Systems, April 2006.

4. Scientific background

4.1 The Barents Sea and the marginal ice zone

The Barents Sea is a shallow shelf sea, with deeper trenches and shallow banks controlling the main currents and associated water mass distributions. The inflow of warm, high-salinity Atlantic Water (AW) from the Norwegian Sea varies on seasonal (Ingvaldsen et al., 2004) as well as interannual time scales (Furevik, 2001). Modified AW exits mainly through the Kara Sea, and from there enters the deep Arctic Ocean. The details of this outflow have been less studied, but available observations show that significant amounts of heat are lost from a large volume of water during the transit of the Barents Sea (Loeng et al., 1997; Schauer et al., 2002). The northern part of the Barents Sea is characterized by inflow of ice and cold, low-salinity Arctic Water (ArW). Satellite observations and model studies have shown this also to be highly variable, controlled primarily by the predominant regional-scale wind regimes (Korsnes et al., 2002; Vinje and Kvambekk, 1991).

The most striking feature within the Barents Sea is the Polar Front, the semi-permanent confluence zone of AW and ArW. The Polar Front follows topography roughly from west to east-southeast but the exact position varies with the dominant inflows and wind systems (Loeng, 1991). The dynamics of the front have been studied in the field (Harris et al., 1998; Parsons et al., 1996) as well as in numerical models (Gawarkiewicz and Plueddemann, 1995). The width, stratification and consequently the steepness of the front have been shown to vary, and the velocities of the along-front currents of AW and ArW origin change in time. In winter the ice edge is usually found near the Polar Front. As ice melts during summer the ice edge gradually moves north (Pfirman et al., 1994), in recent years disappearing more or less completely all the way to the northern shelf break and the entrance to the Kara Sea during late summer. The retreat of the ice edge exposes the underlying water to

sunlight, and, although variable, primary production is known to be intense along the frontal zone (Falk-Petersen et al., 2000).

The marginal ice zone (MIZ) can be loosely defined as the transitional area between open water and dense pack ice (Dixon and Squire, 1995). Ice concentration within the MIZ thus varies between zero and 100%. The range of typical ice floe sizes varies similarly, as waves and swell are free to break the ice up near the outer edge while they are completely dampened in the interior. Here, large floes will primarily be broken up by lateral pressure forces. Also characteristic of the MIZ are the strong local horizontal gradients in wind due to different surface heating and cooling cycles associated with ice and open water, which in turn may force shear currents and upwelling along the outer edge (Guest et al., 1995). In some contexts the term MIZ is used not only to describe the area which at a given time marks the transition between open water and dense ice, but the whole area that goes from being ice covered to ice free during the annual cycle. When this definition is used, all of the northern Barents Sea can be considered an MIZ as all of it at some point will be subject to the characteristic MIZ processes during the annual advance and retreat of the ice.

Since the Barents Sea is shallow (mean depth ~230 m, maximum depth ~500 m), tidal currents are in many places strong. The Spitsbergen Bank in the western part of the Barents Sea in particular so, but this is true also for other shallow banks (Gjevik et al., 1994; Kowalik and Proshutinsky, 1995). Strong tidal mixing and tidal fronts may enhance primary production; the rich fisheries around Sentralbanken, Bear Island and Hopen bear testament to this.

Previous numerical model investigations of the Barents Sea are numerous, including basin-wide studies (e.g. Ådlandsvik and Loeng, 1991; Budgell, 2005; Harms et al., 2005; Slagstad et al., 1990; Støle-Hansen and Slagstad, 1991) as well as simulations of more localized processes (Ådlandsvik and Hansen, 1998; Li and McClimans, 2000; Skogseth et al., 2004, in addition to the Polar Front and tidal simulations mentioned above).

4.2 Turbulence essentials

4.2.1 Physics

Turbulence can be described as the transfer of energy from large to small scales of motion, where the energy is dissipated. Energy is thus converted from velocity (turbulent kinetic energy, TKE) into heat as the motion comes to an end at the molecular level. This energy transfer process ('the energy cascade') is also characterized by efficient redistribution, or diffusion, of the water and its properties – e.g. heat, salt, nutrients and dissolved gases. Turbulence produces significant spatial displacements of water and at the same time exposes large molecular surfaces (per unit time) to each other, allowing efficient transfer of properties. As the water density is determined by its temperature and salinity, vertical redistribution in a stably stratified water column can thus also lead to an increase in potential energy. For more exhaustive descriptions of the characteristics of turbulence, see e.g. Tennekes and Lumley (1972) and Gargett (1997). In the following, the term turbulence refers to homogeneous small-scale three-dimensional turbulence, as opposed to anisotropic turbulence such as larger-scale horizontal eddies (except where specifically noted).

Turbulence arises from instabilities in the field of motion - velocity shear in one or more directions. Small-scale turbulence is often depicted as two-dimensional (2D) eddies or three-dimensional (3D) vortices. Such 'frozen' images can be deceiving though, as it is the transient nature of changing 3D velocity fields and scales itself that defines turbulence. Despite being described as chaotic (in a non-deterministic way), turbulence does adhere to the fundamental laws of nature. Sustained input of energy in the right form is needed to initiate and maintain a state of turbulent motion. In most cases, velocity instability or shear is the main forcing agent. Turbulence can also be driven by convective motion, whereas stabilization of the water column tends to suppress vertical turbulence. In addition to scalar properties of the fluid, the turbulent momentum itself can also be redistributed in space.

The budget of turbulent kinetic energy (TKE) can be formulated as

$$P_{shear} + P_{buoyancy} = DIV + \varepsilon, \quad (1)$$

where P_{shear} is production or input of TKE from velocity shear, $P_{buoyancy}$ is production of TKE by changes in buoyancy (e.g. forced convection by brine release from sea ice (positive contribution) or increased vertical stability due to heating of the surface layer (negative)), DIV is divergence of TKE, while ε is the dissipation of TKE (per unit mass). The divergence term (advection plus diffusion) is usually neglected in cases of fully developed turbulence, which can be assumed to be isotropic (spatially homogeneous).

The concept of the 'turbulent cascade' of energy from the scales of generation to dissipation was elaborated by Kolmogorov (1941a; 1941b). Figure 1 shows an idealized distribution of energy in wavenumber space (wavenumber $k=2\pi/l$, where l is the characteristic length of eddies). The black trace in the figure depicts the power spectral density of the square of turbulent velocities at each wavenumber (more on this later), and the total TKE in this example is the area under the curve; the sum of the energy contributions at the different wavenumbers. The blue curve shows the associated dissipation of energy taking place at different wavenumbers. Most energy is found in the larger eddies and gradually, as eddies interact and become smaller, energy is lost through dissipation. As the size of eddies decreases and the wavenumber corresponding to the scale of molecular viscosity is approached, dissipation reaches a maximum.

Dimensional arguments by Kolmogorov (1941a; 1941b), later supported by observations (Grant et al., 1962, followed by others), show that for fully developed turbulence, the flux of energy is constant through an intermediate part of the cascade; the inertial subrange of the Kolmogorov spectrum. The inertial subrange can be used for diagnostics of the turbulent spectrum. Here, the energy at a given wavenumber is a function of the total dissipation and the wavenumber itself; $E(k)=\alpha\varepsilon^{2/3}k^{-5/3}$ (α is the Kolmogoroff constant). Thus, if the energy in this part of the spectrum can be quantified, so can the total dissipation. An extension to this universal shape of the

inertial subrange, covering the dissipative range of the spectrum, was later formulated through the empirical data of Nasmyth (see Oakey, 1982).

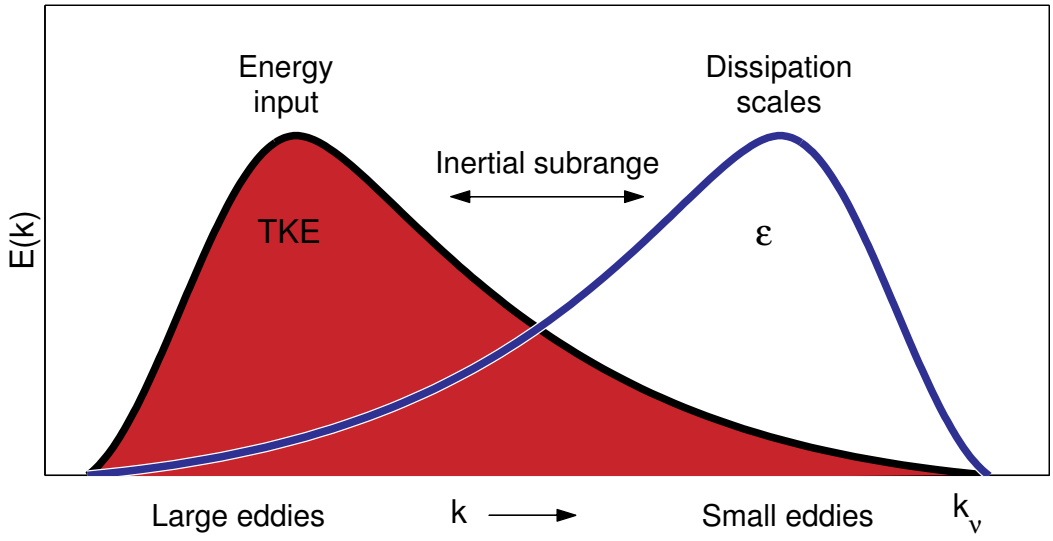

Figure 1. Conceptual energy spectrum showing TKE (red area) and dissipation (blue trace) as functions of wavenumber k. The scales where energy input mainly occurs, from large eddies, are indicated, as well as the dissipative scales. Also shown is the inertial subrange and the wavenumber where viscosity dominates (k_ν). See text for more details.

Given that turbulence is an intermittent process characterized by several non-linear interactions (hence the notion of chaos), it is difficult to predict the exact transfer of energy through the turbulent cascade from singular measurements at the scales of generation. The energy contained in the turbulent cascade is therefore best described by statistical means, by averaging many measurements in time and/or space.

Turbulent motions can be quantified from the small-scale fluctuations in a velocity time series, i.e. the zero-mean deviations from the average flow. If the total velocity (in one direction) at a given time is U and the mean velocity (over a time scale characteristic of large scale current fluctuations) is $\bar{u}$, then the turbulent velocity $u' = U - \bar{u}$ (Reynolds decomposition). Applying the kinetic energy equation $Ek=\frac{1}{2}mv^2$, the turbulent kinetic energy (per unit mass) can then be found from the root-mean-squares (RMS) of the three turbulent velocity components, averaged over an appropriate time interval: $TKE = \frac{1}{2} \langle u'^2 + v'^2 + w'^2 \rangle$ (angle brackets denote

temporal average and u', v' and w' are turbulent velocity components in East, North and vertical directions).

The simplified TKE budget equation (Eq. 1) can be expressed using the Navier-Stokes representation of Newton's Second Law. When filling in for the turbulent components of the flow field after Reynolds decomposition as described above (here given in 2D notation for simplicity), the shear production term in the budget equation can be expressed as $P_{shear} = -\rho_0 < u'w' > \frac{\partial \overline{u}}{\partial z}$, production by buoyancy as $P_{buoyancy} = -\frac{g}{\rho_0} < \rho'w' >$ and dissipation as $\varepsilon = \rho_0 2\nu \left\langle \frac{1}{4}\left(\frac{\partial u'}{\partial z} + \frac{\partial w'}{\partial x} \right)^2 \right\rangle$, where ρ_0 is the reference density, ρ' is the local density perturbation, g is gravitation and ν is molecular viscosity (see e.g. Kantha and Clayson (2000) for more details). These expressions will be explored further in section 4.2.2.

Returning to the turbulent energy cascade, other ways of quantifying turbulent energy and dissipation can be explored. The energy input at larger scales can, at least in principle, be determined by the characteristic scales of the largest eddies in the cascade, where the irreversible transition from mean flow (shear) to eddies destined to break down occurs. It can be shown that the dissipation that eventually results from these eddies should be proportional to the cube of the characteristic velocity, u, and inversely proportional to the length scale (diameter), l, of the largest eddies; $\varepsilon \propto u^3/l$ (Tennekes and Lumley, 1972). According to this, the dissipation does then not depend on the viscosity, i.e. the 'scale' at which molecular dissipation takes place, although this is specific to the fluid being studied.

In a boundary layer, e.g. the surface layer under ice, the scales of turbulence are governed by the distance to the boundary. The amount of turbulent energy that can be fed into such a layer is limited by the maximum size of eddies. This length scale, $\lambda=\kappa z$, is given by the distance z from the boundary and the empirically determined von Karman constant $\kappa \sim 0.4$. This relationship between turbulence energetics and boundary distance is called the law-of-the-wall (LOW) (Karman, 1930; Prandtl,

1932). Furthermore, the stress that generates turbulence within a well mixed surface layer is virtually invariant in space. Given that the stress is constant and the energy available for dissipation is controlled by the distance from the boundary, there must be a relationship between the forcing and the distance from the boundary. The velocity shear, dU/dz, that supplies the forcing to the boundary layer can be expressed as $\frac{dU}{dz} \propto \frac{u_*}{z}$, where u_* is the frictional velocity scale $u_* = (\tau/\rho)^{1/2}$, and τ is the constant shear stress. The LOW can then, through integration, be expressed as $u_* = \kappa U/\ln(z + z_0)$, where z_0 is the surface roughness parameter and κ the (von Karman) constant of integration. If dissipation can be found as $\varepsilon = u^3/l$, the turbulence energetics in a boundary layer can thus be deduced from the external forcing (from dU/dz via u_*) and the interior length scales (here, $l=\lambda$). The above expressions are valid for conditions of neutral stratification and homogeneous turbulence. If the boundary layer is stratified or if there is forced convection the LOW scaling must be modified. Also, LOW is directly applicable only for fixed boundaries such as the sea floor or land-fast or other very densely packed ice, and must be expected to be modified for a partially ice covered surface layer.

In stratified waters, away from boundaries, the size of the largest turbulent eddies is given by the buoyancy scale $l_b = u/N$, where u again is the characteristic velocity scale and N is the buoyancy frequency (from $N^2 = -\frac{g}{\rho_0}\frac{\partial \rho}{\partial z}$). This length scale is the maximum vertical displacement a particle can achieve before all kinetic energy is spent on working against the ambient density field.

A commonly used indicator of turbulence is the Richardson number, Ri, which expresses the relation between vertical stability and shear: $Ri = \frac{N^2}{(\partial u/\partial z)^2}$. Turbulence should not occur for Ri>1/4; for smaller values it may (Howard, 1961; Miles, 1961). The Reynolds number, Re, can also be used to diagnose the state of turbulence in a flow. This is given by Re=LU/ν, where L is the characteristic length scale of the large

scale flow (e.g. depth of surface mixed layer), U is the characteristic velocity of the flow and ν the molecular viscosity. For very small Re no turbulence can be present. Fully developed oceanic turbulence (no non-chaotic structures are left) is found at $Re > 10^5$-10^6. The critical Re value marking the initiation of a turbulent regime in a specific flow depends on the geometrics of the flow (Gargett, 1997).

The motivation for quantifying generation and dissipation of TKE is often the need for assessing the diffusivity – the rate of spreading of properties - in a given system. This is usually expressed by the diffusivity parameter K, which can be used to compute vertical fluxes: $Q=K(dC/dz)$, where dC/dz is the vertical concentration gradient of a given property. If dissipation is known, K can be found from $K=\Gamma\varepsilon/N^2$ (Osborn 1980). Theoretical considerations impose an upper limit on the parameter Γ of 0.20; this value is often used when exact site-specific values for Γ are not known (Gregg 1987). The parameter Γ is related to Rf, the flux Richardson number, such that $\Gamma=Rf/(1-Rf)$. Rf, also called the mixing efficiency, is the ratio of buoyancy production to the input of TKE by shear.

The diffusion coefficient found from dissipation measurements is strictly valid only for calculating diffusion of momentum. For scalars such as heat or salt the effective diffusivity may be different (McPhee, 1992). Nevertheless, referring to Reynolds analogy (for completely isotropic and homogeneous turbulence), the same K value is often applied also for eddy diffusion of e.g. heat and salt.

4.2.2 Measuring turbulence

The energetics of turbulence can be quantified in several ways. In practice, two main approaches have been predominant; 1) measuring micro-scale velocity shear (at the dissipation end of the spectrum), and 2) measuring turbulent velocities (within the inertial subrange of the turbulent cascade).

A fundamental assumption necessary for practical measurements of turbulence in natural waters is Taylor's 'frozen turbulence' hypothesis (Taylor, 1938). This

assumes that the measured time series of a flow-field being advected past a stationary instrument is representative of a point in time, an assumption which is reasonable for many environments. A criterion for applicability is that the turbulent fluctuations should not exceed 10% of the mean advective current velocity. Similarly, for an instrument platform moving through the water the data recorded across the covered spatial range is considered representative of an instantaneous realisation of the turbulent field (again provided that an appropriate averaging interval is used).

Direct measurements at the dissipative scales demand fast-sampling micro-scale resolution (mm-to-cm scale) instrumentation. Such measurements are usually made with free-falling drop-sondes but also with horizontally profiling vehicles moving with constant velocity. Dissipation ε is the sum of the different combinations of directional velocity fluctuations in three dimensions. For measurement purposes one must again assume that the turbulent field is isotropic. The equation for the rate of dissipation per unit mass can then be made uni-directional; $\varepsilon = 7.5\nu\left\langle \left(\partial u'/\partial z\right)^2 \right\rangle$, and measurements of microscale velocity shear along one axis can be utilized (Osborn (1980) based on Batchelor (1953)). As a check of validity of the assumptions, the resulting spectrum can be compared with Nasmyth's universal spectrum of the dissipative range.

In addition to measuring dissipation of TKE, the diffusivity of scalars (e.g. heat, salt), can be used to infer vertical mixing rates. Again assuming isotropy, the dissipation of heat (or more precisely thermal variance) is found from $\chi = 2k_T \left\langle 3\left(\partial T'/\partial z\right)^2 \right\rangle$, where k_T is the molecular diffusivity for heat and $\partial T'/\partial z$ is the small-scale vertical fluctuations of temperature (Osborn and Cox, 1972).

From fixed-position small-scale 3D velocity time series measurements, the turbulent velocities are found through Reynolds decomposition, applying linear detrending if necessary. In practice, the production of TKE from shear can be found from the Reynolds stress components (<u'w'> etc, see expression for P_{shear} in section 4.2.1).

Dissipation at a given wavenumber (k) in the inertial subrange of the spectrum can be estimated from the turbulent velocity components by utilizing the Kolmogorov relationship, $\sigma_{uu}(k)=\alpha\varepsilon^{2/3}k^{-5/3}$, where α is Kolmogorov's constant and $\sigma_{uu}(k)$ is the spectral density of one velocity component (McPhee, 2004). The variance spectrum can be calculated either through Fourier transformation of the time series or from zero-lag autocorrelation of the velocity components.

If measurements of the small-scale fluctuations of scalars are made in parallel to those of velocity fluctuations, vertical fluxes can be calculated with the 'eddy-correlation method'. Vertical heat flux, for example, can be found as $Q_h=\rho C_p\langle w'T'\rangle$, where ρ is density and C_p is specific heat of seawater. This method has been used with data both from fixed-point time series (McPhee, 1992) and from vertical profiling (Moum, 1996a).

Collection of time-series of 3D velocity with the necessary spatial and temporal resolution and quality is often difficult due to motion of the observation platform (ship, mooring) and has therefore been most successfully performed with mast-mounted instrumentation at sea ice camps or in the bottom-boundary layer.

Measurements at the scales where energy is fed into the turbulent cascade (e.g. from $\varepsilon \propto u^3/l$, as discussed in section 4.2.1) may be more easily accomplished than in the inertial or dissipative ranges. While the complexity of the cascade and the fact that several different length scales may be involved in the generation process make such 'inviscid estimates' difficult, some success has been achieved (Moum, 1996b).

Complementary to the 'direct' measurements of the energetics of turbulence described above, much can be learned about the temporal mean mixing in the oceans through tracer release experiments (e.g. Ledwell et al., 1998).

During the Cabanera project both the drop-sonde and fixed-point techniques have been used. The former measurements became the most comprehensive and successful and it is the results of these that are presented in Papers I and II.

4.2.3 Representing turbulence in numerical ocean models

The thickness of vertical grid cells in numerical ocean circulation models are typically of order 1-10 m in the surface layer, increasing with depth. The range of scales spanning the spectrum of turbulence (mm to cm) is therefore not resolved. Representation of turbulence must then be parameterized in some way, as a function of forcing by larger scale features. Knowledge of the triggering processes and efficiency of transferring kinetic energy to vertical mixing is necessary for these models to get fundamental aspects of the ocean circulation correct; surface mixed layer evolution, deep water formation, heat exchange between ice and ocean etc.

In the infancy of ocean modelling, an area-mean diffusivity value (K) was used for the whole water column. Simple fixed-value K-profiles were suggested, and later a linear dependence on stability N was introduced (Gargett and Holloway, 1984). Over the last decades, several different ways of modelling the transfer from large scale forcing to turbulent dissipation and diffusion have been proposed, and representations in which the diffusivity is a function of shear and stratification (and other parameters) are now generally applied in 3D ocean models. These can be classified in three main groups:

1) Richardson number parameterizations. This straightforward approach assesses the competing influences of stratification and vertical velocity shear. Typically, if stratification is strong compared with current shear between two neighbouring vertical cells (e.g. Ri >1/4) a modest ‘background’ diffusivity is used. For intermediate Ri values the diffusivity K becomes directly dependent on Ri through some sort of shape function. At very low Ri numbers (e.g. when stratification is neutral), a maximum diffusivity value is ascribed. The Richardson number approach can be classified as a first-order diagnostic representation. The concept was first suggested by Munk and Anderson (1948), and applications similar to that of Pacanowski and Philander (1981) are still used in many models. Different supplementary processes, such as the effect of wind waves in the surface layer, can be added.

2) Boundary layer theory models (or first-order closure schemes). The model proposed by Large et al. (1994), often referred to as the KPP or K-profile parameterization, has proven useful particularly for deep open ocean applications. The diffusion coefficient in the surface layer is a function of the depth of the boundary layer (h), the turbulent velocity scale (w) and a shape function G: $K(\sigma)=h\, w(\sigma)G(\sigma)$, where $\sigma=z/h$ is a non-dimensional vertical coordinate. The boundary layer depth is determined as the minimum of either an Ekman depth calculation or a depth defined by a critical bulk Richardson number (based on shear between surface velocity and sub-surface horizontal velocity as calculated by the model, and the local stratification). The velocity scale is based on atmospheric surface boundary layer similarity theory, and is given as a function of the friction velocity u_*, the Monin-Obukhov length scale L (which in turn depends on surface buoyancy flux), a stability-dependent non-dimensional flux function and depth. The coefficients of the third order polynomial shape function G are determined from boundary conditions at the surface and below the mixed layer. For the depth ranges below the surface boundary layer, a Ri scheme can be used.

3) Turbulence closure schemes. These more complex schemes are based on the Navier-Stokes equation for the Reynolds components, as described by Mellor and Yamada (1982). The full (Level 4) model consists of 11 partial differential equations for second moments of the turbulent velocity terms. Such a model is very exerting on computer resources. Several simplifications to the non-linear terms, based on scaling arguments, were proposed and shown not to decrease the accuracy of the model unacceptably (relative to other uncertainties). The resulting Mellor-Yamada (MY) Level 2.5 scheme is now widely used. Like the two previous model types, the MY scheme also uses vertical gradients of velocity and density to determine values for diffusivity, but does so prognostically by closing the energy budget for the water column using physical length scales determined by distance to the boundaries. This scheme advects and diffuses the TKE driving the mixing, and diffuses the signals in

time. The eddy diffusion parameter is found as K=qlS, where q is the turbulent kinetic energy, l is the turbulent macro scale, and S is a stability function given by l^2, q^2, stratification and various empirically determined constants. The differential equations yielding q and l are of the same form as the prognostic equations for temperature and salinity but using q^2 and q^2l as variables for which to solve. The so-called k-ε turbulence models are also based on the Navier-Stokes equations. These somewhat less complex models also relate the turbulent fluxes of momentum and buoyancy to the vertical gradients of velocity and density. The closure of the resulting equations is made through an eddy viscosity term $\nu_t=cq^2/\varepsilon$ (c is a constant) and boundary conditions with a wall proximity correction (Burchard and Baumert, 1995).

The choice of how to represent turbulence in a particular model application depends on the vertical resolution and discretization that is used. Also, the horizontal grid extent and time scale over which simulations will be made influence the computational demands and thus also the complexity of the diffusion scheme. In Paper 3, simulations were made with both the Ri scheme which has been routinely used in the SINMOD model so far, and the MY Level 2.5 model. Performance of the two methods is compared and evaluated against observational data on turbulent mixing from selected locations (from Papers 1 and 2).

As computational capacity increases, model resolution can be increased and it should be possible to cover at least part of the spectrum of turbulence. In principle one should then be able to describe the evolution from forcing through the turbulent cascade to dissipation by means of the Navier-Stokes equation of motion for fluids, as this should contain all the forces governing the turbulent motions. Several issues render this approach difficult. The initiation of turbulence – the transition from laminar (directionally uniform) to turbulent flow – has been described as a threshold process (e.g. occurring above a certain Re or below a Ri value). Determination of this threshold is not trivial. Also, although the net energy flux in the cascade is towards

smaller eddies, observations have shown that small eddies may interact and merge into larger ones.

Large eddy simulations (LES) go one step further than the standard schemes used in large-scale ocean models. Here, explicit simulations of the large energy-containing eddies within the spectrum of turbulence are made through the Navier-Stokes equations. These eddies are directly influenced by the large scale flow, while the smaller eddies adhere to the more universal shape of the inertial and dissipative ranges and are parameterized as a function of the larger eddies. While credible results come out of simulations for isotropic homogeneous turbulence, problems arise when stratification is introduced, or in the proximity of boundaries (Lesieur and Metais, 1996). Efforts at computing the full range of scales in turbulence are made with so-called direct numerical simulations (DNS). Full Navier-Stokes computations including even the dissipative scales are made with the aid of spectral techniques. This approach can at present be used only for very small spatial domains and is limited to Reynolds numbers smaller than those observed in most oceanic environments (Moin and Mahesh, 1998). Information from LES and DNS simulations has provided insight into the non-linear interactions within the turbulent cascade, which are difficult to observe both in nature and laboratories (e.g. Li et al., 2005; Tse et al., 2004). Even if this level of resolution cannot be incorporated in large-scale 3D ocean models yet, such simulations can increase our fundamental understanding of turbulence, and be useful for improving the parameterizations of the sub-grid scale processes.

4.2.4 Effects of turbulence on biogeochemical processes

In addition to the direct effects of physically mixing the water itself, turbulence affects biology on different scales from the physiology of individual organisms to the functioning of species and ecosystems. Vertical mixing controls the distribution of both particulate matter and dissolved constituents including gases such as CO_2. The following non-exhaustive (and unscaled!) list illustrates the range over which

turbulence influences these coupled systems (Davis et al., 1991; Gargett, 1997; Gargett and Marra, 2002; Ross, 2006; Rothschild and Osborn, 1988; Visser and MacKenzie, 1998, and references therein).

1) Turbulence provides vertical exchange of nutrients. The rate at which nutrients are supplied to the euphotic layer through the stratified intermediate waters and pycnocline effectively controls gross productivity.

2) Phytoplankton will be vertically redistributed and thus exposed to variable irradiance. The temporal and spatial scales of turbulence thus affects species adversely as their response and tolerance to different light intensities may be different.

3) The encounter rates between predators and their prey can depend on local turbulence. The feeding success and preferences of e.g. zooplankton preying on phytoplankton and fish larvae on zooplankton will change with different exposure to turbulence. And vice versa, the prey might have to adapt its behaviour to enhance the likelihood of survival.

4) Similarly, the intermittent and patchy nature of turbulence can aggregate or disperse plankton, changing both their access to nutrients/food and their susceptibility to being preyed upon. Higher density of organisms can be observed both as horizontal patches and vertical layers.

5) Phytoplankton, relying on exchanges with their environment through permeable cell walls, can be affected by the intensity of turbulence at the smallest dissipative scales. When total TKE input increases, the size of turbulent eddies becomes ever smaller to enable the system to dissipate more energy. Concentration gradients associated with skin effects near the membranes of organisms can then change, affecting flux rates.

6) Turbulence affects suspension/sinking rates of particulate organic matter (POM) such as detritus. The resulting vertical distribution determines where in

the water column the POM is dissolved and remineralised. Also, turbulent motion can physically break up detritus thus changing sinking velocities and increasing the surface available for consumption by bacteria.

7) The vertical distribution of dissolved gases is controlled through air-sea exchange and by mixing internally in the water column. Fluxes between the surface mixed layer and the pycnocline and on to the deep water, and finally between deep water and benthos, are all determined by turbulent mixing (and the concentrations in the different layers).

8) The concentrations of the CO_2 system constituents are also affected indirectly, e.g. through effects on the biological carbon utilization and through turbulent heat fluxes acting on the ice cover which controls the air-sea exchange.

9) The larger scale budget of CO_2; e.g. whether the Barents Sea acts as a net sink of atmospheric CO_2, depends on the water mass modification taking place in the area. If large volumes of intermediate or deep waters are formed during times of the year when the atmospheric partial pressure of CO_2 is greater than that of the (surface) ocean, a net export of dissolved carbon into the neighbouring deep oceans may be the result. Such water mass formation can be controlled by turbulence in frontal zones between different water masses and along the ice edge.

5. Summaries of papers

5.1 Paper I. Observations of turbulent mixing and hydrography in the marginal ice zone of the Barents Sea

During the CABANERA cruises in 2004 and 2005, measurements were made at eight ice drift stations in the northern Barents Sea MIZ. Descriptions of hydrography, ice drift, currents, wind, and model predictions of barotropic tidal currents for the stations are given. The main topic of the paper is vertical mixing within and below the pycnocline. Turbulence inferred from microstructure shear measurements was observed to vary significantly between stations, and enhanced turbulent dissipation could be attributed to strong current shear between the surface and sub-surface layers. Strong tidal flow over shallow topography induced strong mixing throughout the water column. At stations with strong wind forcing increased mixing was seen to protrude into the pycnocline. Ice drift stations with little wind forcing and without strong current shear had station-mean dissipation up to a factor 50 lower than at the high-energy stations. In such areas double diffusive (DD) staircases were identified and the contribution from DD convection to the vertical heat flux could be quantified. High-resolution CTD measurements were used to isolate density overturns, from which turbulent length scales can be calculated. Averaged over a large number of overturns these data were used to quantify dissipation of turbulent kinetic energy, found to be in good agreement with that found from the microstructure shear measurements. Different parameterizations of dissipation as function of current shear variability and water column stability indicated that internal waves were not likely to be a major contributor to production of turbulent mixing. A simple shear-stratification parameterization tuned with survey-mean dissipation reproduced the observed variability reasonably well.

5.2 Paper II. Observations of upper ocean boundary layer dynamics in the marginal ice zone

This paper describes the surface boundary layer dynamics of the CABANERA drift stations in May 2005. Ice-ocean shear was found to dominate the turbulent kinetic energy budget for the surface layer, while ice melting contributed to stabilization. Wind work calculated from shipborne measurements as well as work done by stress under the ice was significantly correlated with integrated dissipation in the mixing layer. In the upper part of the under-ice mixing layer the observed dissipation profiles were enhanced compared with a standard constant-stress wall layer scaling. An alternative scaling, accounting for the effect of ice floe keels, reproduced the upper half of the mixed layer dissipation profile better. Variability of mixed layer dissipation was best described when using local friction speed and the mixing length profile was adjusted for buoyancy fluxes. Changes to the depth to which enhanced mixing and thus entrainment of pycnocline water takes place were strongly correlated with the friction speed. Turbulent heat fluxes as large as 300-500 W m^{-2} were inferred for the mixing layers above warm Atlantic Water, in agreement with values obtained from an independent parameterization.

5.3 Paper III. Vertical mixing in the MIZ of the northern Barents Sea – results from numerical model experiments

A 3D ocean circulation model was used for simulation of the northern Barents Sea marginal ice zone (MIZ) during the three CABANERA project years, 2003-2005. A description of modelled seasonal development of water mass stability and vertical mixing is given, with special emphasis on the melting period, characterized by strong stratification, shallow surface mixed layers and low diffusivities. Large-scale features simulated by the model such as ice cover and inflow of heat with Atlantic Water are found to be in good agreement with available observations. Comparison of modelled diffusivity with measurements from the CABANERA ice drift stations shows that diffusivity profiles from diverse periods spanning low-energy settings, high wind speeds and areas with strong tidal currents can be satisfactorily reproduced numerically. Observed hydrography profiles, however, suggest that the model over time overestimates the depth of the surface mixed layer and the strength of the pycnocline, and that deep water masses may be mixed excessively. The model has until now applied a Richardson-number based vertical mixing scheme. Simulations with the Mellor-Yamada Level 2.5 scheme produced results similar to those from the Ri-scheme, although some differences were identified. Model simulations were also made with increased horizontal and vertical grid resolution. When reducing the cell size from 4×4 km^2 km to 800×800 m^2, horizontal processes near the edge of the MIZ produced vertical exchanges and enhanced sub-surface diffusivities. Having identified differences between observations and model simulations, possible adaptations of the mixing schemes for improved performance in the MIZ are explored. Different boundary layer length scale modifications can be applied, with the aim of reducing near-surface and deep mixing. The presence of double diffusivity and internal waves in the area support applying a larger minimum mixing coefficient in the model, which would enhance pycnocline diffusivity. Parameterizations of wind-wave and ice keel effects should also be considered.

6. Conclusions

Highly variable mixing has been observed in the Barents Sea marginal ice zone, covering a wide range of forcing (strong winds and spring tides as well as calmer conditions) and water column stability (from the surface mixed layer to strong seasonal pycnoclines). Analyses of the observations have revealed that

- under-ice keels affect the vertical distribution of dissipation within the mixing layer
- mixing internally in and deepening of the surface mixed layer can be diagnosed as a function of wind and buoyancy flux, using a modified Law-of-the-Wall parameterization
- diffusivities within the pycnocline can to some extent be described by total current kinetic energy in the corresponding depth interval
- breaking of internal waves does not appear to be a dominant agent for upper-ocean vertical mixing in the marginal ice zone of the interior Barents Sea
- in regions of weak physical forcing, double-diffusive convection can be important for upward heat fluxes and water mass modification

Through comparison of hydrography and diffusivities from observations with numerical ocean model experiments we have found that

- individual episodes of wind and tides (and calm conditions) can be reproduced by the model, and the general distributions of water masses and ice cover are in agreement with observations
- over time, the effect of surface mixing can extend too deep, the pycnocline may be too strong, and near-bottom mixing often homogenizes the deep part of the water column too effectively in the model

- the modelled development of diffusivity shows significant seasonal changes; high diffusivities during winter, when stratification is weak, via a minimum during the melting period when large quantities of melt water are introduced, to an increase in the ice-free season when wind-driven mixing is more efficient and only solar heating provides additional buoyancy

- both the Richardson-number based mixing scheme and the Mellor-Yamada Level 2.5 scheme reproduce the general water mass distributions and seasonal development from winter to summer, but neither is found to reproduce the observed MIZ hydrography optimally

- increasing the horizontal resolution from 4 km to 800 m allows for important ice edge processes to be resolved in the model

7. Future perspectives

For a more complete understanding of the turbulent processes in the MIZ to be achieved, more comprehensive studies of vertical mixing need to be made. A larger survey should comprise fixed-point turbulence measurements as well as near-continuous microstructure profiling. The profiling should preferably be made with rising-mode instruments to capture the immediate under-ice boundary layer. More complete coverage of the forcing mechanisms than what we were able to do in this project is needed, e.g. by means of fine-resolution current profilers lowered from the survey vessel, from ice floes and on bottom moorings. Only through comprehensive dedicated efforts can we hope to delineate the integrated effects of different forcing mechanisms in this ice-covered environment. This is crucial for proper evaluation of numerical model performance and further development of these with respect to vertical mixing.

Recent findings indicate that substantial vertical mixing may be induced by the ocean's life forms themselves; Dewar et al. (2006) have presented budgets of the possible contribution of biologically induced turbulence to the large-scale interior ocean mixing, arguing that this could well be of the same magnitude as that of wind or tides (thus providing the "missing" mixing needed to balance deep stratification and the meridional overturning circulation!). Their focus was on the interior ocean (>200 m) but biological turbulence might be important in the upper ocean as well. Here, density and tracer concentration gradients are often steeper and the small-scale turbulence induced by the smaller and more abundant trophic levels can be efficient. During low-wind conditions and away from the strongest current shear it may be that e.g. zooplankton and schools of fish are the primary drivers of enhanced pycnocline mixing (Huntley and Zhou, 2004). Kunze et al. (2006) found that vertically migrating krill enhanced local turbulence by three to four orders of magnitude during their ascent, thereby increasing averaged mixing by a factor of 100. This is certainly an issue that merits further study. When measuring turbulence in highly productive areas such as the blooming MIZ, where large zooplankton is abundant (albeit not

necessarily migrating diurnally), biologically generated turbulence should be targeted as a specific topic of study. Microstructure measurements should anyway be made more routinely during inter-disciplinary field campaigns, for better interpretation of bio-geo measurements and more generally to expand the database on oceanic turbulence.

The representation of turbulence in regional scale ocean models needs further refinement. An intermediate step between observations and 3D modelling is to test the performance of different mixing schemes in 1D modelling systems such as the General Ocean Turbulence Model (Burchard et al., 2006). Here, available observations of wind, currents, hydrography and turbulence can be used for testing of different model parameterizations in an efficient manner before suggestions for improvement are tested in 3D models. A larger measurement program should have a strategy involving such an evaluation phase before making recommendations for improvement for the larger regional ocean models.

References

Ådlandsvik, B. and Hansen, R., 1998. Numerical simulation of the circulation in the Svalbardbanken area in the Barents Sea. Continental Shelf Research, 18(2-4): 341-355.

Ådlandsvik, B. and Loeng, H., 1991. A Study of the Climatic System in the Barents Sea. Polar Research, 10(1): 45-49.

Batchelor, B.K., 1953. The theory of homogeneous turbulence. Cambridge University Press, Cambridge, 197 pp.

Budgell, P., 2005. Numerical simulation of ice-ocean variability in the Barents Sea region: Towards dynamical downscaling. Ocean Dynamics, 55(3-4): 370-387.

Burchard, H. and Baumert, H., 1995. On the performance of a mixed-layer model based on the *k*-ε turbulence closure. Journal of Geophysical Research, 100(C5): 8523-8540.

Burchard, H. et al., 2006. Description of a flexible and extendable physical-biogeochemical model system for the water column. Journal of Marine Systems, 61(3-4): 180-211.

Craig, P.D. and Banner, M.L., 1994. Modeling wave-enhanced turbulence in the ocean surface layer. Journal of Physical Oceanography, 24(12): 2546-2559.

Crawford, G., Padman, L. and McPhee, M., 1999. Turbulent Mixing in Barrow Strait. Continental Shelf Research, 19: 205-245.

Davis, C.S., Flierl, G.R., Wiebe, P.H. and Franks, P.J.S., 1991. Micropatchiness, turbulence and recruitment in plankton. Journal of Marine Research, 49: 109-151.

Dewar, W.K. et al., 2006. Does the marine biosphere mix the ocean? Journal of Marine Research, 64(4): 541-561.

Dixon, T.W. and Squire, V.A., 1995. Energy transport in the marginal ice zone. Journal of Geophysical Research, 106(C9): 19917-19927.

Ezer, T., 2000. On the seasonal mixed layer simulated by a basin-scale ocean model and the Mellor-Yamada turbulence scheme. Journal of Geophysical Research, 105(C7): 16843-16855.

Falk-Petersen, S. et al., 2000. Physical and ecological processes in the marginal ice zone of the northern Barents Sea during the summer melt period. Journal of Marine Systems, 27(1-3): 131-159.

Furevik, T., 2001. Annual and interannual variability of Atlantic Water temperatures in the Norwegian and Barents Seas: 1980-1996. Deep-Sea Research I, 48(2): 383-404.

Gargett, A.E., 1997. "Theories" and techniques for observing turbulence in the ocean euphotic zone. Scientia Marina, 61: 25-45.

Gargett, A.E. and Holloway, G., 1984. Dissipation and diffusion by internal wave breaking. Journal of Marine Research, 42: 15-27.

Gargett, A.E. and Marra, J., 2002. Effects of upper ocean physical processes (turbulence, advection and air-sea interaction) on oceanic primary production. In: A.R. Robinson, J.J. McCarthy and B.J. Rothschild (Editors), The Sea. John Wiley & Sons, Inc., New York, pp. 19-49.

Gargett, A.E. and Moum, J.N., 1995. Mixing efficiencies in Turbulent Tidal Fronts: Results from Direct and Indirect Measurements of Density Flux. Journal of Physical Oceanography, 25(11): 2583-2608.

Gawarkiewicz, G. and Plueddemann, A.J., 1995. Topographic Control of Thermohaline Frontal Structure in the Barents Sea Polar Front on the South Flank of Spitsbergen Bank. Journal of Geophysical Research-Oceans, 100(C3): 4509-4524.

Gjevik, B., Nøst, E. and Straume, T., 1994. Model simulations of the tides in the Barents Sea. Journal of Geophysical Research-Oceans, 99(C2): 3337-3350.

Grant, H.L., Stewart, R.W. and Molliet, A., 1962. Turbulence spectra from a tidal channel. Journal of Fluid Mechanics, 12: 241-268.

Gregg, M.C., 1987. Diapycnal Mixing in the Thermocline: A Review. Journal of Geophysical Research-Oceans, 92(C5): 5249-5286.

Gregg, M.C., 1989. Scaling Turbulent Dissipation in the Thermocline. Journal of Geophysical Research-Oceans, 94(C7): 9686-9698.

Guest, P.S., Glendening, J.W. and Davidson, K.L., 1995. An observational and numerical study of wind stress variations within marginal ice zones. Journal of Geophysical Research, 100(C6): 10887-10904.

Harms, I., Schrum, C. and Hatten, K., 2005. Numerical sensitivity studies on the variability of climate-relevant processes in the Barents Sea. Journal of Geophysical Research, 110, C06002, doi:10.1029/2004JC002559.

Harris, C.L., Plueddemann, A.J. and Gawarkiewicz, G.G., 1998. Water mass distribution and polar front structure in the western Barents Sea. Journal of Geophysical Research-Oceans, 103(C2): 2905-2917.

Howard, L.N., 1961. Note on a paper of John W. Miles. Journal of Fluid Mechanics, 10(4): 509-513.

Huntley, M. and Zhou, M., 2004. Influence of animals on turbulence in the sea. Marine Ecology Progress Series, 273: 65-79.

Ingvaldsen, R., Asplin, L. and Loeng, H., 2004. The seasonal cycle in the Atlantic transport to the Barents Sea during the years 1997–2001. Continental Shelf Research, 24: 1015-1032.

Kantha, L.H. and Clayson, C.A., 2000. Small scale processes in geophysical fluid flows. International Geophysics Series, 67. Academic Press, San Diego, Cal, 888 pp.

Karman, 1930. Mechanische Ahnlichkeit und turbulenz. Nachr. Ges. Wiss. Gottingen, Math. Phys., K1: 58-76.

Kolmogorov, A.N., 1941a. Dissipation of energy in locally isotropic turbulence. Dokl. Akad. Nauk SSSR, 32: 16:18 (Reprinted in Proc. Roy. Soc. Lond. A, 434:15:17,1991).

Kolmogorov, A.N., 1941b. The local structure of turbulence in incompressible viscous fluid for very large Reynolds number. Dokl. Akad. Nauk SSSR, 30: 9:13 (Reprinted in Proc. Roy. Soc. Lond. A, 434: 15:17, 1991).

Korsnes, R., Pavlova, O. and Godtliebsen, F., 2002. Assessment of potential transport of pollutants into the Barents Sea via sea ice - an observational approach. Marine Pollution Bulletin, 44(9): 861-869.

Kowalik, Z. and Proshutinsky, A.Y., 1995. Topographic enhancement of tidal motion in the western Barents Sea. Journal of Geophysical Research, 100(C2): 2613-2637.

Kunze, E., Dower, J.F., Beveridge, I., Dewey, R. and Bartlett, K.P., 2006. Observations of Biologically Generated Turbulence in a Coastal Inlet. Science, 313(5794): 1768-1770.

Large, W.G., McWilliams, J.C. and Doney, S.C., 1994. Oceanic vertical mixing: A review and a model with a nonlocal boundary layer parameterization. Reviews of Geophysics, 32(4): 363-403.

Ledwell, J.R., Watson, A.J. and Law, C.S., 1998. Mixing of a tracer in the pycnocline. Journal of Geophysical Research-Oceans, 103(C10): 21499-21529.

Lesieur, M. and Metais, O., 1996. New trends in large-eddy simulations of turbulence. Annual Review of Fluid Mechanics, 28: 45-82.

Li, M., Sanford, L. and Chao, S.Y., 2005. Effects of time dependence in unstratified tidal boundary layers: results from large eddy simulations. Estuarine, Coastal and Shelf Science, 62(1-2): 193-204.

Li, S. and McClimans, T.A., 2000. On the stability of barotropic prograde and retrograde jets along a bottom slope. Journal of Geophysical Research, 105(C4): 8847-8855.

Loeng, H., 1991. Features of the Physical Oceanographic Conditions of the Barents Sea. Polar Research, 10(1): 5-18.

Loeng, H., Ozhigin, V. and Ådlandsvik, B., 1997. Water fluxes through the Barents Sea. Ices Journal of Marine Science, 54(3): 310-317.

McPhee, M., 2004. A Spectral Technique for Estimating Turbulent Stress, Scalar Flux Magnitude, and Eddy Viscosity in the Ocean Boundary Layer under Pack Ice. J. Phys. Oceanogr., 34(10): 2180-2188.

McPhee, M.G., 1992. Turbulent heat flux in the upper ocean under sea ice. Journal of Geophysical Research, 97(C4): 5365-5379.

Mellor, G.L., 2003. The Three-Dimensional Current and Surface Wave Equations. Journal of Physical Oceanography, 33(9): 1978–1989.

Mellor, G.L. and Yamada, H., 1982. Development of a turbulence closure model for geophysical fluid problems. Reviews of Geophysics and Space Physics, 20: 851-875.

Miles, J.W., 1961. On the stability of heterogeneous shear flows. Journal of Fluid Mechanics, 10(4): 496-515.

Moin, P. and Mahesh, K., 1998. Direct numerical simulation: A tool in turbulence research. Annual Review of Fluid Mechanics, 30: 539-578.

Morison, J.H., McPhee, M. and Maykut, G.A., 1987. Boundary Layer, Upper Ocean, and Ice Observations in the Greenland Sea Marginal Ice Zone. Journal of Geophysical Research, 92(C7): 6987-7011.

Moum, J.N., 1996a. Efficiency of mixing in the main thermocline. J. Geophys. Res., 101(12): 12,057-12,069.

Moum, J.N., 1996b. Energy-containing scales of turbulence in the ocean thermocline. Journal of Geophysical Research, 101(C6): 14095-14109.

Munk, W., 1966. Abyssal recipes. Deep-Sea Research, 13: 707-730.

Munk, W.H. and Anderson, E.R., 1948. Notes on the theory of the thermocline. Journal of Marine Research, 7(3): 276-295.

Oakey, N.S., 1982. Determination of the Rate of Dissipation of Turbulent Energy from Simultaneous Temperature and Velocity Shear Microstructure Measurements. Journal of Physical Oceanography, 12(3): 256-271.

Osborn, T.R., 1980. Estimates of the Local Rate of Vertical Diffusion from Dissipation Measurements. Journal of Physical Oceanography, 10(1): 83-89.

Osborn, T.R. and Cox, C.S., 1972. Oceanic Fine Structure. Geophysical Fluid Dynamics, 3: 321-345.

Pacanowski, R.C. and Philander, G.H., 1981. Parameterization of vertical mixing in numerical models of tropical oceans. Journal of Physical Oceanography, 11: 1443-1451.

Padman, L. and Dillon, T.M., 1991. Turbulent Mixing Near the Yermak Plateau During the Coordinated Eastern Arctic Experiment. Journal of Geophysical Research-Oceans, 96(C3): 4769-4782.

Parsons, A.R. et al., 1996. The Barents Sea Polar Front in summer. Journal of Geophysical Research-Oceans, 101(C6): 14201-14221.

Pfirman, S.L., Bauch, D. and Gammelsrød, T., 1994. The Northern Barents Sea: Water Mass Distribution and Modification. In: O.M. Johannessen, R.D. Muench and J.E. Overland (Editors), The Polar Oceans and Their Role in Shaping the Global Environment: The Nansen Centennial Volume. AGU, Washington DC, pp. 77-94.

Polzin, K.L., Toole, J.M., Ledwell, J.R. and Schmitt, R.W., 1997. Spatial variability of turbulent mixing in the abyssal ocean. Science, 276(5309): 93-96.

Prandtl, L., 1932. Zur turbulenten stromung in rohren und langs platten. Ergebn. Aerodyn. Versuchanst Gottingen, 4: 18-29.

Qiao, F. et al., 2004. Wave-induced mixing in the upper ocean: Distribution and application to a global ocean circulation model. Geophysical Research Letters, 31, L11303, doi:10.1029/2004GL019824.

Ross, O.N., 2006. Particles in motion: How turbulence affects plankton sedimentation from an oceanic mixed layer. Geophysical Research Letters, 33(L10609): doi:10.1029/2006GL026352.

Rothschild, B.J. and Osborn, T.R., 1988. Small-Scale Turbulence and Plankton Contact Rates. Journal of Plankton Research, 10(3): 465-474.

Schauer, U., Loeng, H., Rudels, B., Ozhigin, V.K. and Dieck, W., 2002. Atlantic Water flow through the Barents and Kara Seas. Deep-Sea Research I, 49(12): 2281-2298.

Sharples, J., Moore, C.M. and Abraham, E.R., 2001. Internal tide dissipation, mixing, and vertical nitrate flux at the shelf edge of NE New Zealand. Journal of Geophysical Research, 106(C7): 14069-14081.

Simpson, J.H., Crawford, W.R., Rippeth, T.P., Campbell, A.R. and Cheok, J.V.S., 1996. The Vertical Structure of Turbulent Dissipation in Shelf Seas. Journal of Physical Oceanography, 26(8): 1579-1590.

Skogseth, R., Haugan, P.M. and Haarpaintner, J., 2004. Ice and brine production in Storfjorden from four winters of satellite and in situ observations. Journal of Geophysical Research-Oceans, 109, C10008, doi:10.1029/2004JC002384.

Slagstad, D., Støle-Hansen, K. and Loeng, H., 1990. Density Driven Currents in the Barents Sea Calculated by a Numerical Model. Modeling, Identification and Control, 11(4): 181-190.

Støle-Hansen, K. and Slagstad, D., 1991. Simulation of currents, ice melting, and vertical mixing in the Barents Sea using a 3-D baroclinic model. Polar Research, 10(1): 33-44.

Taylor, G.I., 1938. The Spectrum of Turbulence. Proc. Roy. Soc. Lond. A, 164(919): 476 - 490.

Tennekes, H. and Lumley, J.L., 1972. A First Course in Turbulence. MIT Press, Cambridge, Mass., 300 pp.

Tse, K.L., Mahalov, A., Nicolaenko, B. and Joseph, B., 2004. High resolution DNS of shear-convective turbulence and its implications to second-order parameterizations. Theoretical and Computational Fluid Dynamics, 17(5-6): 445-462.

Vinje, T. and Kvambekk, Å.S., 1991. Barents Sea drift ice characteristics. Polar Research, 10(1): 59-68.

Visser, A.W. and MacKenzie, B.R., 1998. Turbulence induced contact rates of plankton: the question of scale. Marine Ecology Progress Series, 166: 307-310.